Porosity area fraction analysis of bonded borosilicate specimens from in-situ optical imagery

Peter W. Spaeth[1], Matthew R. Webster[2]

Nondestructive Evaluation Sciences Branch
NASA Langley Research Center
Hampton, VA 23681
(757) 8648622; fax (757) 8644914; email [1]peter.w.spaeth@nasa.gov, [2]matthew.r.webster@nasa.gov

ABSTRACT

Image segmentation methods are routinely used to analyze data derived in nondestructive testing scenarios. A typical problem in this area is to estimate porosity from X-ray Computed Tomography (CT) inspections. This investigation aims to understand the effectiveness of open-source image segmentation methods for porosity estimation from optical images in the context of strength analysis of bonded materials and provides a benchmark of performance against a standard commercial software package. The rank ordering of the specimens by porosity area fraction is consistent across both methods.

Keywords: Porosity area fraction, image analysis, image segmentation, random forest classifier, borosilicate bonded composite

INTRODUCTION

Borosilicate specimens were bonded under varying conditions as part of an adhesive strength study [1] that applied Ultrasonic Testing (UT) and a modeling approach introduced in [2, 3]. The mass density and elastic properties of the adhesive are important components in the spring-mass model used to assess bond-strength, and these parameters are also directly impacted by porosity. The impacts of porosity on the effective speed of sound can be estimated using a variety of methods, a concise summary of which is given by Ramakrishnan [4]. Accurate values for the porosity area fraction and pore size distribution are essential for applying these methods in practice.

In this work the porosity of the bond-line was estimated using optical images of the post-cured borosilicate specimens. Images of the specimens were captured using an off the shelf digital camera focused on the bond plane while the specimens were backlit to highlight pores in the adhesive. The image processing technique that was used to estimate porosity area fraction (i.e., porosity per unit area) utilizes an image segmentation algorithm based on random forests. This technique was trained on a small subset of manually labeled data and then evaluated on all specimens. Repeated training and application of the model provided estimates of the porosity fraction of each specimen, and a representative segmentation that yields the porosity area fraction that is closest to the mean was used to estimate equivalent spherical pore diameter. Finally, the results were compared against estimates obtained using the Defect Detection module of the commercial software suite VG STUDIO MAX.

METHODOLOGY

Numerous commercial and open-source libraries exist for image processing tasks such as image segmentation. In this study the approach to segmentation based on random forests from Scikit-image [5] was applied to the four images in the middle row of **Figure 1**. Under this approach features based on pixel intensity, edges, and textures are first computed from the input images. Then masks, identified in each image corresponding to different classes, are used to train a random forest classifier that ultimately assigns classes to all unlabeled pixels.

The analysis was carried out on regions of interest within the bonded section of the specimens to avoid the Kapton tape and its interface with the bonded region. A small number of pores and solid regions were labeled in each region of interest for training. Due to varying lighting conditions and contrast across the images, the training and evaluation were carried out separately on each specimen. The regions of interest for each of the four specimens are shown in **Figure 1**. To understand the dependence of the porosity-area estimate on the training of the classifier, the random

forest segmentation algorithm was applied 100 times for each specimen. The segmentation with porosity area fraction closest to the mean value across the 100 evaluations is shown in the bottom row of **Figure 1**.
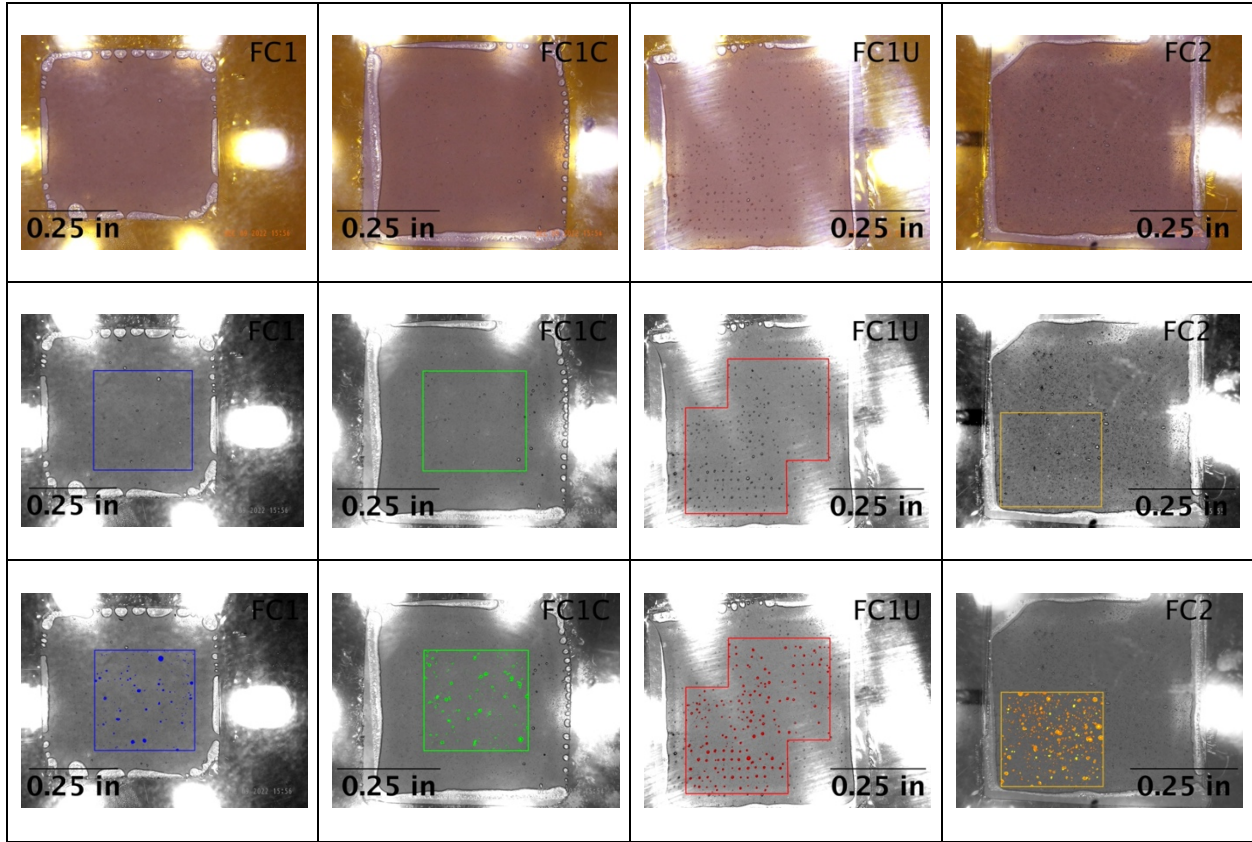

Figure 1: (Top row) Images of the four bonded borosilicate specimens with varying amounts of porosity. The bonded region occupies an approximately 0.5 in by 0.5 in square-shaped region. The orange region surrounding the bond in each specimen is due to Kapton tape that was applied to create a barrier to hold the adhesive and bright spots are due to the backlighting of the specimens. Specimen ID is shown in each image. (Middle row) Grayscale images of the four specimens. (Bottom row) The segmentation nearest the mean value estimated for each specimen.

RESULTS

The estimate of porosity area fraction in each specimen's region of interest was evaluated for each of the 100 trials, and the results are combined in Error! Reference source not found.. The approach using a camera shows the differences in porosity across the specimens. For example, the analysis shows that specimen FC2 contains the greatest porosity area fraction.
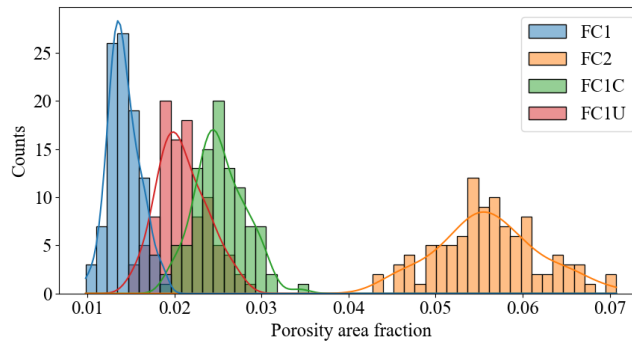

Figure 2. Porosity fraction estimates for each of the 100 applications of the random forest segmentation algorithm. Analysis of the optical images enables differentiation of the porosity area fraction between the samples.

For each specimen, its mean segmentation was used to evaluate pore size. To provide a quantitative analysis of the pore diameter of each specimen, equivalent spherical diameter was estimated using a two-parameter exponential distribution with scale $1/\lambda$ and location γ, i.e., with probability density function

$$f(x) = \lambda \exp(-\lambda(x - \gamma)).$$

Maximum likelihood estimates for the location and scale parameters based on the mean segmentation for each specimen are given in **Table 1**.

Table 1: Parameter estimates for equivalent spherical diameter across specimens.

Specimen	FC1	FC1C	FC1U	FC2
Location: γ (in)	0.000898	0.000779	0.000779	0.000726
Scale: $1/\lambda$ (in)	0.001792	0.001710	0.003686	0.001760
Mean: $1/\lambda + \gamma$ (in)	0.002690	0.002488	0.004465	0.002485

The distribution of pore diameters across specimens using the mean segmentations is shown in **Figure 3**. Specimen FC1U stands out among the four samples in that its mean pore diameter is nearly double the value of the other three. This specimen was unique in that it was cured at a lower temperature and for a shorter time than the other specimens in order to achieve an "under-cured" state. Differences in the viscosity of the adhesive at the lower temperature may have affected the degassing process.
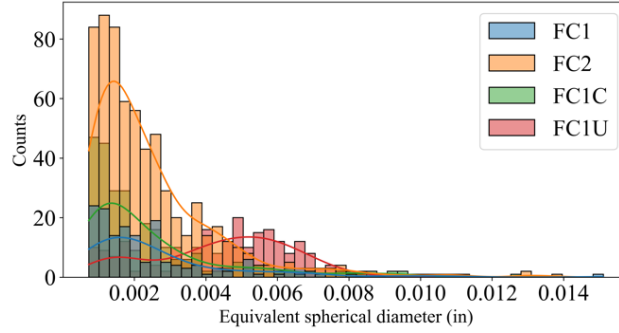

Figure 3. Equivalent spherical diameter of all pores identified in the mean segmentation of each specimen. Analysis of the optical images enables quantification of the equivalent spherical diameter of the pores between the samples.

To benchmark the results derived from Scikit-image, VG STUDIO MAX was also used to estimate porosity area fraction from the grayscale images of the specimens. The built-in function VGDefX was used. Single point estimates of porosity area fraction from VG STUDIO MAX and mean-values of the results derived by Scikit-image show the same rank-ordering of the specimens in terms of porosity area fraction. The greatest difference in the two approaches was observed in Specimen FC2.

Table 2: Porosity fraction estimates using Scikit-image and VG STUDIO MAX.

	FC1	FC1C	FC1U	FC2
Scikit-image	0.014201	0.025266	0.020894	0.056025
VG STUDIO MAX	0.0185	0.0228	0.0219	0.0679

Finally, the segmentations derived from Scikit-image and VGSTUDIO MAX in the region of interest for specimen FC1C are compared using the two methods. Specimen FC1C's region of interest and corresponding segmentations obtained from Scikit-image and VG STUDIO MAX are shown in **Figure 4**.
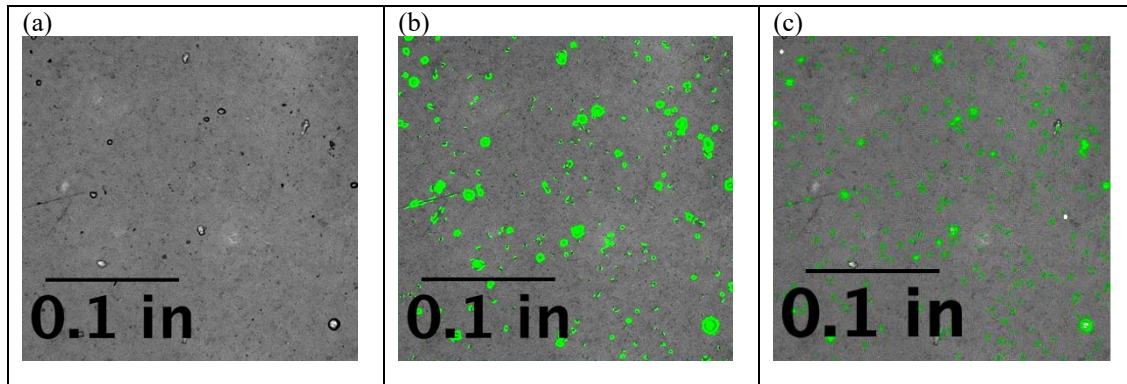
Figure 4: Comparison of (a) original optical image of specimen FC1C cropped to the region of interest, (b) its Scikit-image segmentation, and (c) segmentation obtained from VGSTUDIO MAX.

CONCLUSIONS

Accurate porosity analysis is critical for the nondestructive evaluation of bonded structures. The results of this analysis show that open-source methods such as those in Scikit-image can be used to quantify the differences in porosity among a cohort of bonded specimens. Across the four borosilicate specimens that were analyzed, preliminary results indicate compatibility between these porosity estimates and the ultrasound results from [1]. Specifically, interaction with the adhesive caused a generally larger phase shift in more porous specimens owing to the impact of porosity on wave speed. Moreover, the comparison between Scikit-image results and those derived from VG STUDIO MAX showed the same rank-ordering of the specimens in terms of increasing porosity area fraction. Similar results were also observed for estimating pore diameter using Scikit-image and VG STUDIO MAX. Quantifying the dependence of porosity area on the location and size of the region of interest will be an important next step in the bond-strength analysis. Validating the porosity area estimates will also help characterize the accuracy of estimating porosity from optical images rather than from X-ray CT inspections of the borosilicate specimens.

REFERENCES

[1] M. R. Webster and P. Takunju, "Phase Based Ultrasonic Inspection of Degraded Adhesive Joints," in *Proceedings of ASNT Research Symposium*, Columbus, OH, 2023.

[2] J. Cantrell, "Assessment of adhesive bond strength from ultrasonic tone-bursts," *J Nondestr Eval,* vol. 37, no. 4, 2018.

[3] H. Haldren, W. T. Yost, D. Perey, K. E. Cramer and M. C. Gupta, "A constant-frequency ultrasonic phase method for monitoring imperfect adherent/adhesive interfaces," *Ultrasonics,* vol. 120, no. 106641, 2022.

[4] N. Ramakrishnan, "Speed of Sound in Porous Materials," *Bull. Mater. Sci.,* vol. 17, pp. 499-504, 1994.

[5] S. v. d. Walt, J. L. Schönberger, J. Nunez-Iglesias, F. Boulogne, J. D. Warner, N. Yager, E. Gouillart and T. Yu, "scikit-image: image processing in Python," *PeerJ,* vol. 2, no. e453, 2014.